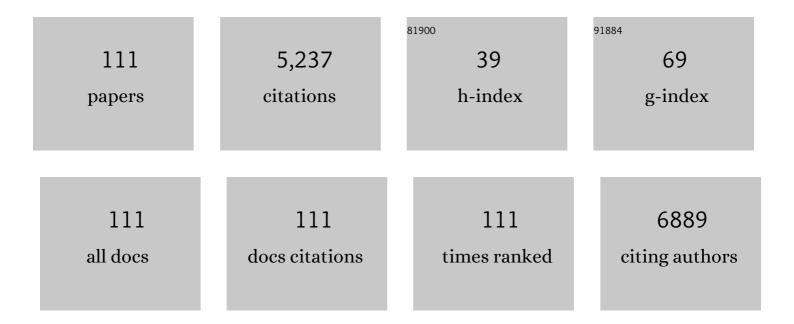
List of Publications by Year in descending order

Source: https://exaly.com/author-pdf/1043966/publications.pdf Version: 2024-02-01



#	Article	IF	CITATIONS
1	An Early Wave of Macrophage Infiltration Intertwined with Antigen-Specific Proinflammatory T Cells and Browning of Adipose Tissue Characterizes the Onset of Orbital Inflammation in a Mouse Model of Graves' Orbitopathy. Thyroid, 2022, 32, 283-293.	4.5	11

2 Dynamic monitoring of vital functions and tissue re-organization in Saturnia pavonia (Lepidoptera,) Tj ETQq0 0 0 rgBT /Overlock 10 Tf 50

3	A Toolbox to Investigate the Impact of Impaired Oxygen Delivery in Experimental Disease Models. Frontiers in Medicine, 2022, 9, .	2.6	2
4	Multiparametric MRI identifies subtle adaptations for demarcation of disease transition in murine aortic valve stenosis. Basic Research in Cardiology, 2022, 117, .	5.9	6
5	Phenotyping placental oxygenation in Lgals1 deficient mice using 19F MRI. Scientific Reports, 2021, 11, 2126.	3.3	4
6	Endothelial β1 Integrin-Mediated Adaptation to Myocardial Ischemia. Thrombosis and Haemostasis, 2021, 121, 741-754.	3.4	10
7	4-hydroxytamoxifen does not deteriorate cardiac function in cardiomyocyte-specific MerCreMer transgenic mice. Basic Research in Cardiology, 2021, 116, 8.	5.9	9
8	Dapagliflozin reduces thrombin generation and platelet activation: implications for cardiovascular risk reduction in type 2 diabetes mellitus. Diabetologia, 2021, 64, 1834-1849.	6.3	22
9	Endothelial hyaluronan synthase 3 aggravates acute colitis in an experimental model of inflammatory bowel disease. Matrix Biology, 2021, 102, 20-36.	3.6	5
10	Does timing matter in radiotherapy of hepatocellular carcinoma? An experimental study in mice. Cancer Medicine, 2021, 10, 7712-7725.	2.8	9
11	Endothelial Hyaluronan Synthase 3 Augments Postischemic Arteriogenesis Through CD44/eNOS Signaling. Arteriosclerosis, Thrombosis, and Vascular Biology, 2021, 41, 2551-2562.	2.4	7
12	Beyond Vessel Diameters: Non-invasive Monitoring of Flow Patterns and Immune Cell Recruitment in Murine Abdominal Aortic Disorders by Multiparametric MRI. Frontiers in Cardiovascular Medicine, 2021, 8, 750251.	2.4	5
13	Multi-targeted 1H/19F MRI unmasks specific danger patterns for emerging cardiovascular disorders. Nature Communications, 2021, 12, 5847.	12.8	31
14	Acute Heart Failure After Reperfused Ischemic Stroke: Association With Systemic and Cardiac Inflammatory Responses. Frontiers in Physiology, 2021, 12, 782760.	2.8	5
15	In vivo clearance of 19F MRI imaging nanocarriers is strongly influenced by nanoparticle ultrastructure. Biomaterials, 2020, 261, 120307.	11.4	33
16	Fluorineâ€19 Magnetic Resonance Imaging of Activated Platelets. Journal of the American Heart Association, 2020, 9, e016971.	3.7	14
17	MRI-based molecular imaging of epicardium-derived stromal cells (EpiSC) by peptide-mediated active targeting. Scientific Reports, 2020, 10, 21669.	3.3	4
18	Anaemia is associated with severe RBC dysfunction and a reduced circulating NO pool: vascular and cardiac eNOS are crucial for the adaptation to anaemia. Basic Research in Cardiology, 2020, 115, 43.	5.9	34

#	Article	IF	CITATIONS
19	Hot spot ¹⁹ F magnetic resonance imaging of inflammation. Wiley Interdisciplinary Reviews: Nanomedicine and Nanobiotechnology, 2020, 12, e1639.	6.1	23
20	Phagocytosis of a PFOB-Nanoemulsion for 19F Magnetic Resonance Imaging: First Results in Monocytes of Patients with Stable Coronary Artery Disease and ST-Elevation Myocardial Infarction. Molecules, 2019, 24, 2058.	3.8	20
21	A2bR-dependent signaling alters immune cell composition and enhances IL-6 formation in the ischemic heart. American Journal of Physiology - Heart and Circulatory Physiology, 2019, 317, H190-H200.	3.2	11
22	4-Methylumbelliferone improves the thermogenic capacity of brown adipose tissue. Nature Metabolism, 2019, 1, 546-559.	11.9	26
23	Special issue on fluorine-19 magnetic resonance: technical solutions, research promises and frontier applications. Magnetic Resonance Materials in Physics, Biology, and Medicine, 2019, 32, 1-3.	2.0	7
24	Cardiac Hyaluronan Synthesis Is Critically Involved in the Cardiac Macrophage Response and Promotes Healing After Ischemia Reperfusion Injury. Circulation Research, 2019, 124, 1433-1447.	4.5	47
25	Longitudinal 19F magnetic resonance imaging of brain oxygenation in a mouse model of vascular cognitive impairment using a cryogenic radiofrequency coil. Magnetic Resonance Materials in Physics, Biology, and Medicine, 2019, 32, 105-114.	2.0	7
26	In vivo 19F MR inflammation imaging after myocardial infarction in a large animal model at 3ÂT. Magnetic Resonance Materials in Physics, Biology, and Medicine, 2019, 32, 5-13.	2.0	22
27	Dissociation of 19F and fluorescence signal upon cellular uptake of dual-contrast perfluorocarbon nanoemulsions. Magnetic Resonance Materials in Physics, Biology, and Medicine, 2019, 32, 133-145.	2.0	22
28	Targeting sphingosine-1-phosphate lyase as an anabolic therapy for bone loss. Nature Medicine, 2018, 24, 667-678.	30.7	93
29	Multimodal assessment of orbital immune cell infiltration and tissue remodeling during development of graves disease by ¹ H ¹⁹ F MRI. Magnetic Resonance in Medicine, 2018, 80, 711-718.	3.0	12
30	IL-23R Signaling Plays No Role in Myocardial Infarction. Scientific Reports, 2018, 8, 17078.	3.3	1
31	Simultaneous Assessment of Cardiac Inflammation and Extracellular Matrix Remodeling After Myocardial Infarction. Circulation: Cardiovascular Imaging, 2018, 11, .	2.6	30
32	Insulin Resistance and Vulnerability to Cardiac Ischemia. Diabetes, 2018, 67, 2695-2702.	0.6	31
33	Synthetic Cargo Internalization Receptor System for Nanoparticle Tracking of Individual Cell Populations by Fluorine Magnetic Resonance Imaging. ACS Nano, 2018, 12, 11178-11192.	14.6	18
34	Graves' orbitopathy occurs sex-independently in an autoimmune hyperthyroid mouse model. Scientific Reports, 2018, 8, 13096.	3.3	24
35	State of the Art in Cardiovascular T2 Mapping: on the Way to a Cardiac Biomarker?. Current Cardiovascular Imaging Reports, 2018, 11, 1.	0.6	5
36	Nrf2 Deficiency Unmasks the Significance of Nitric Oxide Synthase Activity for Cardioprotection. Oxidative Medicine and Cellular Longevity, 2018, 2018, 1-15.	4.0	34

#	Article	IF	CITATIONS
37	Echocardiographic Analysis of Cardiac Function after Infarction in Mice: Validation of Single-Plane Long-Axis View Measurements and the Bi-Plane Simpson Method. Ultrasound in Medicine and Biology, 2018, 44, 1544-1555.	1.5	21
38	Biomedical 19F MRI Using Perfluorocarbons. Methods in Molecular Biology, 2018, 1718, 235-257.	0.9	5
39	A novel physiological role for cardiac myoglobin in lipid metabolism. Scientific Reports, 2017, 7, 43219.	3.3	29
40	CD73 on T Cells Orchestrates Cardiac Wound Healing After Myocardial Infarction by Purinergic Metabolic Reprogramming. Circulation, 2017, 136, 297-313.	1.6	68
41	Mechanisms of Insulin Resistance in Primary and Secondary Nonalcoholic Fatty Liver. Diabetes, 2017, 66, 2241-2253.	0.6	124
42	Opening of calcium-activated potassium channels improves long-term left-ventricular function after coronary artery occlusion in mice. International Journal of Cardiology, 2017, 241, 351-357.	1.7	3
43	Cardiovascular Magnetic Resonance Relaxometry Predicts Regional Functional Outcome After Experimental Myocardial Infarction. Circulation: Cardiovascular Imaging, 2017, 10, .	2.6	16
44	Characterization of perfluorocarbon relaxation times and their influence on the optimization of fluorine-19 MRI at 3 tesla. Magnetic Resonance in Medicine, 2017, 77, 2263-2271.	3.0	25
45	Impact of dietary nitrate on age-related diastolic dysfunction. European Journal of Heart Failure, 2016, 18, 599-610.	7.1	20
46	Epicardium-Derived Cells Formed After Myocardial Injury Display Phagocytic Activity Permitting In Vivo Labeling and Tracking. Stem Cells Translational Medicine, 2016, 5, 639-650.	3.3	22
47	Myocardial T2 Mapping Increases NoninvasiveÂDiagnostic Accuracy for Biopsy-Proven Myocarditis. JACC: Cardiovascular Imaging, 2016, 9, 1467-1469.	5.3	30
48	lron-regulatory proteins secure iron availability in cardiomyocytes to prevent heart failure. European Heart Journal, 2016, 38, ehw333.	2.2	115
49	Chapter 4 Active Targeting of Perfluorocarbon Nanoemulsions. , 2016, , 103-140.		2
50	Fluorine MR Imaging of Inflammation in Atherosclerotic Plaque in Vivo. Radiology, 2015, 275, 421-429.	7.3	50
51	Myocardial T2 mapping reveals age- and sex-related differences in volunteers. Journal of Cardiovascular Magnetic Resonance, 2015, 17, 9.	3.3	77
52	Sexual dimorphism of lipid metabolism in very long-chain acyl-CoA dehydrogenase deficient (VLCADâ^'/â^') mice in response to medium-chain triglycerides (MCT). Biochimica Et Biophysica Acta - Molecular Basis of Disease, 2015, 1852, 1442-1450.	3.8	18
53	Noninvasive Imaging of Early Venous Thrombosis by ¹⁹ F Magnetic Resonance Imaging With Targeted Perfluorocarbon Nanoemulsions. Circulation, 2015, 131, 1405-1414.	1.6	79
54	Loss of UCP2 Attenuates Mitochondrial Dysfunction without Altering ROS Production and Uncoupling Activity. PLoS Genetics, 2014, 10, e1004385.	3.5	63

#	Article	IF	CITATIONS
55	Technical Advance: Monitoring the trafficking of neutrophil granulocytes and monocytes during the course of tissue inflammation by noninvasive 19F MRI. Journal of Leukocyte Biology, 2014, 95, 689-697.	3.3	33
56	RIP3, a kinase promoting necroptotic cell death, mediates adverse remodelling after myocardial infarction. Cardiovascular Research, 2014, 103, 206-216.	3.8	257
57	Visualization of immune cell infiltration in experimental viral myocarditis by 19F MRI in vivo. Magnetic Resonance Materials in Physics, Biology, and Medicine, 2014, 27, 101-106.	2.0	38
58	Probing different perfluorocarbons for <i>in vivo</i> inflammation imaging by ¹⁹ F MRI: image reconstruction, biological half-lives and sensitivity. NMR in Biomedicine, 2014, 27, 261-271.	2.8	138
59	Multifunctional MR monitoring of the healing process after myocardial infarction. Basic Research in Cardiology, 2014, 109, 430.	5.9	28
60	Development and pathomechanisms of cardiomyopathy in very long-chain acyl-CoA dehydrogenase deficient (VLCADâ~'/â^') mice. Biochimica Et Biophysica Acta - Molecular Basis of Disease, 2014, 1842, 677-685.	3.8	40
61	Lack of ecto-5′-nucleotidase (CD73) promotes arteriogenesis. Cardiovascular Research, 2013, 97, 88-96.	3.8	20
62	Ecto-5′-Nucleotidase on Immune Cells Protects From Adverse Cardiac Remodeling. Circulation Research, 2013, 113, 301-312.	4.5	42
63	Deletion of CD73 promotes dyslipidemia and intramyocellular lipid accumulation in muscle of mice. Archives of Physiology and Biochemistry, 2013, 119, 39-51.	2.1	22
64	Development of a Growing Rat Model for the InÂVivo Assessment of Engineered Aortic Conduits. Journal of Surgical Research, 2012, 176, 367-375.	1.6	42
65	Selective Activation of Adenosine A _{2A} Receptors on Immune Cells by a CD73-Dependent Prodrug Suppresses Joint Inflammation in Experimental Rheumatoid Arthritis. Science Translational Medicine, 2012, 4, 146ra108.	12.4	111
66	¹⁹ F magnetic resonance imaging of endogenous macrophages in inflammation. Wiley Interdisciplinary Reviews: Nanomedicine and Nanobiotechnology, 2012, 4, 329-343.	6.1	97
67	Fluorine-19 Magnetic Resonance Angiography of the Mouse. PLoS ONE, 2012, 7, e42236.	2.5	25
68	Methods Employed for Induction and Analysis of Experimental Myocardial Infarction in Mice. Cellular Physiology and Biochemistry, 2011, 28, 1-12.	1.6	48
69	Noninvasive Detection of Graft Rejection by In Vivo 19F MRI in the Early Stage. American Journal of Transplantation, 2011, 11, 235-244.	4.7	61
70	Modified Suture Technique in a Mouse Heart Transplant Model. Asian Journal of Surgery, 2011, 34, 86-91.	0.4	6
71	Disrupted fat distribution and composition due to medium-chain triglycerides in mice with a Î ² -oxidation defect. American Journal of Clinical Nutrition, 2011, 94, 439-449.	4.7	30
72	MR for the Investigation of Murine Vasculature. Methods in Molecular Biology, 2011, 771, 439-456.	0.9	1

#	Article	IF	CITATIONS
73	In vitro differentiation of unrestricted somatic stem cells into functional hepaticâ€like cells displaying a hepatocyteâ€like glucose metabolism. Journal of Cellular Physiology, 2010, 225, 545-554.	4.1	29
74	Early Assessment of Pulmonary Inflammation by ¹⁹ F MRI In Vivo. Circulation: Cardiovascular Imaging, 2010, 3, 202-210.	2.6	108
75	Keeping the heart in balance: the functional interactions of myoglobin with nitrogen oxides. Journal of Experimental Biology, 2010, 213, 2726-2733.	1.7	52
76	Decreased contractility due to energy deprivation in a transgenic rat model of hypertrophic cardiomyopathy. Journal of Molecular Medicine, 2009, 87, 411-422.	3.9	34
77	The natriuretic peptide/guanylyl cyclase–A system functions as a stress-responsive regulator of angiogenesis in mice. Journal of Clinical Investigation, 2009, 119, 2019-2030.	8.2	95
78	Myoglobin tames tumor growth and spread. Journal of Clinical Investigation, 2009, 119, 766-768.	8.2	4
79	Nitrosative Stress Leads to Protein Glutathiolation, Increased S-Nitrosation, and Up-regulation of Peroxiredoxins in the Heart. Journal of Biological Chemistry, 2008, 283, 17440-17449.	3.4	31
80	Survivin Determines Cardiac Function by Controlling Total Cardiomyocyte Number. Circulation, 2008, 117, 1583-1593.	1.6	105
81	In Vivo Monitoring of Inflammation After Cardiac and Cerebral Ischemia by Fluorine Magnetic Resonance Imaging. Circulation, 2008, 118, 140-148.	1.6	306
82	Overexpression of prostaglandin EP3 receptors activates calcineurin and promotes hypertrophy in the murine heart. Cardiovascular Research, 2008, 81, 310-318.	3.8	26
83	The Osmolyte Taurine Protects against Ultraviolet B Radiation-Induced Immunosuppression. Journal of Immunology, 2007, 179, 3604-3612.	0.8	35
84	Nitrite Reductase Function of Deoxymyoglobin. Circulation Research, 2007, 100, 1749-1754.	4.5	270
85	In vivo 2D mapping of impaired murine cardiac energetics in NO-induced heart failure. Magnetic Resonance in Medicine, 2007, 57, 50-58.	3.0	39
86	Direct comparison of magnetic resonance imaging and conductance microcatheter in the evaluation of left ventricular function in mice. Basic Research in Cardiology, 2006, 101, 87-95.	5.9	48
87	SGK1-dependent cardiac CTGF formation and fibrosis following DOCA treatment. Journal of Molecular Medicine, 2006, 84, 396-404.	3.9	111
88	Chronic liver disease is triggered by taurine transporter knockout in the mouse. FASEB Journal, 2006, 20, 574-576.	0.5	106
89	Cardiospecific Overexpression of the Prostaglandin EP3Receptor Attenuates Ischemia-Induced Myocardial Injury. Circulation, 2005, 112, 400-406.	1.6	40
90	Oxygen supply and nitric oxide scavenging by myoglobin contribute to exercise endurance and cardiac function. FASEB Journal, 2005, 19, 1015-1017.	0.5	46

#	Article	IF	CITATIONS
91	Lack of Myoglobin Causes a Switch in Cardiac Substrate Selection. Circulation Research, 2005, 96, e68-75.	4.5	57
92	Monitoring left ventricular dilation in mice with PET. Journal of Nuclear Medicine, 2005, 46, 1516-21.	5.0	14
93	Taurine transporter knockout depletes muscle taurine levels and results in severe skeletal muscle impairment but leaves cardiac function uncompromised. FASEB Journal, 2004, 18, 577-579.	0.5	156
94	Targeted Disruption of <i>cd73</i> /Ecto-5′-Nucleotidase Alters Thromboregulation and Augments Vascular Inflammatory Response. Circulation Research, 2004, 95, 814-821.	4.5	220
95	Role of myoglobin in the antioxidant defense of the heart. FASEB Journal, 2004, 18, 1156-1158.	0.5	140
96	Adaptation of the myoglobin knockout mouse to hypoxic stress. American Journal of Physiology - Regulatory Integrative and Comparative Physiology, 2004, 286, R786-R792.	1.8	28
97	Acute Inhibition of Myoglobin Impairs Contractility and Energy State of iNOS-Overexpressing Hearts. Circulation Research, 2003, 92, 1352-1358.	4.5	59
98	Myoglobin Protects the Heart from Inducible Nitric-oxide Synthase (iNOS)-mediated Nitrosative Stress. Journal of Biological Chemistry, 2003, 278, 21761-21766.	3.4	76
99	Cardiac-Specific Overexpression of Inducible Nitric Oxide Synthase Does Not Result in Severe Cardiac Dysfunction. Circulation Research, 2002, 90, 93-99.	4.5	134
100	Myoglobin facilitates oxygen diffusion. FASEB Journal, 2001, 15, 1077-1079.	0.5	92
101	Myoglobin facilitates oxygen diffusion. FASEB Journal, 2001, 15, 1077-1079.	0.5	32
102	Effects of Ammonia Exposition on Glioma Cells: Changes in Cell Volume and Organic Osmolytes Studied by Diffusion-Weighted and High-Resolution NMR Spectroscopy. Developmental Neuroscience, 2000, 22, 463-471.	2.0	54
103	Contribution of NO to Ischemia-Reperfusion Injury in the Saline-Perfused Heart: a Study in Endothelial NO Synthase Knockout Mice. Journal of Molecular and Cellular Cardiology, 1999, 31, 827-836.	1.9	90
104	Alterations in glial cell metabolism during recovery from chronic osmotic stress. Neurochemical Research, 1998, 23, 1553-1561.	3.3	5
105	A1H/13C inverse 2D method for the analysis of the polyamines putrescine, spermidine and spermine in cell extracts and biofluids. , 1998, 11, 47-54.		29
106	Rat brain primary neurons immobilized in basement membrane gel threads: an improved method for on-line NMR spectroscopy of live cells. Brain Research Protocols, 1998, 3, 183-191.	1.6	6
107	Assessment of the Mechanism of Astrocyte Swelling Induced by the Macrolide Immunosuppressant Sirolimus Using Multinuclear Nuclear Magnetic Resonance Spectroscopy. Chemical Research in Toxicology, 1997, 10, 1359-1363.	3.3	24
108	Determination ofde novo synthesized amino acids in cellular proteins revisited by13C NMR spectroscopy. , 1997, 10, 50-58.		8

#	Article	IF	CITATIONS
109	Adaptation of Cellular Metabolism to Anisosmotic Conditions in a Glial Cell Line, as Assessed by ¹³ C-NMR Spectroscopy. Developmental Neuroscience, 1996, 18, 449-459.	2.0	14
110	Immobilization of Primary Astrocytes and Neurons for On-Line Monitoring of Biochemical Processes by NMR. Developmental Neuroscience, 1996, 18, 478-483.	2.0	19
111	Regulation of intracellular pH in neuronal and glial tumour cells, studied by multinuclear NMR spectroscopy. NMR in Biomedicine, 1994, 7, 157-166.	2.8	42